Received: 21 April 2022 | Revised: 7 June 2022 | Accepted: 8 June 2022

DOI: 10.1002/dvdy.507

TECHNIQUES

Developmental Dynamics WILEY

A method to investigate muscle target-specific transcriptional signatures of single motor neurons

Bianka Berki | **Fabio Sacher** | **Antoine Fages** | **Patrick Tschopp** | **Maëva Luxey**

DUW Zoology, University of Basel, Basel, Switzerland

Correspondence
Maëva Luxey, DUW Zoology, University of Basel, Vesalgasse 1, CH-4051, Basel, Switzerland.
Email: maeva.luxey@unibas.ch

Funding information
Forschungsfonds of the University of Basel; Schweizerischer Nationalfonds zur Förderung der Wissenschaftlichen Forschung, Grant/Award Number: 31003A_170022; Stiftung für die Erforschung der Muskelkrankheiten; Universität Basel; Swiss National Science Foundation; *Olga Mayenfisch Stiftung*

Abstract

Background: Motor neurons in the vertebrate spinal cord have long served as a paradigm to study the transcriptional logic of cell type specification and differentiation. At limb levels, pool-specific transcriptional signatures first restrict innervation to only one particular muscle in the periphery, and get refined, once muscle connection has been established. Accordingly, to study the transcriptional dynamics and specificity of the system, a method for establishing muscle target-specific motor neuron transcriptomes would be required.

Results: To investigate target-specific transcriptional signatures of single motor neurons, here we combine ex-ovo retrograde axonal labeling in mid-gestation chicken embryos with manual isolation of individual fluorescent cells and Smart-seq2 single-cell RNA-sequencing. We validate our method by injecting the dorsal *extensor metacarpi radialis* and ventral *flexor digiti quarti* wing muscles and harvesting a total of 50 fluorescently labeled cells, in which we detect up to 12,000 transcribed genes. Additionally, we present visual cues and cDNA metrics predictive of sequencing success.

Conclusions: Our method provides a unique approach to study muscle target-specific motor neuron transcriptomes at a single-cell resolution. We anticipate that our method will provide key insights into the transcriptional logic underlying motor neuron pool specialization and proper neuromuscular circuit assembly and refinement.

KEYWORDS

axonal backfill, limb motor neuron-muscle connection, manual cell picking, neural tube dissociation, single motor neuron sequencing, Smart-seq2

1 | INTRODUCTION

During Metazoan development, a multitude of various cell types need to be specified to ensure proper functioning of the body. The central nervous system represents one prime example of this emergent cellular complexity. Indeed, in vertebrates, the spinal cord is composed of a high number of molecularly distinct cell

types, interconnected with each other and also with their target organs.[1]

In this context, limb innervating spinal motor neurons are particularly interesting. During their maturation, they go through a series of sub-differentiation steps after which their molecular footprint directly reflects the affinity of their axons toward one particular muscle in the limb periphery.[2,3] They first gain lateral motor column (LMC) identity at the levels of the limb, and thereafter split into lateral and medial LMCs, to ensure dorsal and ventral limb innervation, respectively. Subsequently, they subdivide into so-called motor neuron pools that are spatially segregated from one another, and represent transcriptionally unique sets of neurons innervating one specific muscle.[4-6] To date, only few motoneuron pool-specific genes have been identified, and our knowledge of the developmental specification and muscle target-induced refinement of pool-specific transcriptomes remains incomplete.

The recent development and commercialization of emulsion-based single-cell RNA-sequencing technologies have greatly contributed to our understanding of spinal neuronal subtype specification during development, as well as their distinct molecular signatures in adult individuals.[7-11] However, studying motor neuron pool diversification with these high-throughput methods remains difficult, due to tissue dissociation-induced loss of spatial information and more importantly muscle target-connectivity.[12] Moreover, despite recent studies aiming to account for target connectivity in a high throughput manner,[13-16] the need for a more specific and user-defined method to purify single motor neurons from a given pool, still connected to their cognate muscle within an embryonic time-frame, becomes apparent to study target-specific neuronal transcriptomes with appropriate resolution.

Retrograde axonal labeling has long been used to map the connection between target muscles and the position of the corresponding motor neuron cell bodies in the spinal cord.[17-19] This method consists of injecting a tracer molecule into the target muscle of choice, and let it be transported to the soma of the connected motor neurons in the spinal cord. This method has successfully been applied to create topological maps of limb muscle innervation in chicken embryos.[17,20] Unfortunately, the low number of labeled cell bodies resulting from this method makes the FACS-based (fluorescent-activated cell sorting) isolation of those cells for transcriptional profiling almost impossible. Alternatively, laser-capture microscopy has been used to excise labeled cells from sections of the spinal cord, yet this method does not result in single-cell resolution transcriptomes.[21]

Here, we present an optimized workflow combining ex-ovo fluorescent retrograde axonal labeling followed by manual cell selection, to investigate the transcriptomic signatures of individual motor neurons connected to a specific peripheral muscle target (Figure 1). Our protocol provides details on optimal culture conditions for mid-gestation chicken embryos, focal injection into a single peripheral muscle, spinal cord dissociation, manual purification, and visual inspection of fluorescent cells from plated neurons followed by the highly sensitive Smart-seq2 single-cell RNA-sequencing. As a proof of principle, we purify motor neurons from the pools innervating the *extensor metacarpi radialis* (EMR) and *flexor digiti quarti* (FDQ), two muscles on opposite extremes along with the three axes of the limb, that is, dorso-ventral, proximo-distal, and antero-posterior. In total, we isolate 50 purified EMR- and FDQ-connected cells that were sequenced following the Smart-seq2 protocol.[22] After assessing the overall quality of the cellular transcriptomes and filtering based on the expression levels of mitochondrial genes as an indicator of cellular stress, we reliably detect—in cells with satisfying cDNA profiles—the expression of 8000 to 12,000 genes per cellular transcriptome, including several motor neuron-specific markers.

Collectively, we present a method that provides transcriptomic data from muscle-specific embryonic motor neuron pools at single-cell resolution. Our method has the potential to provide key insights into the transcriptional status of forming motor neuron pools that are connecting to their cognate muscles. Moreover, our technique opens new avenues to elucidate the molecular crosstalk between nerves and muscles that underlies neuromuscular circuit establishment and refinement.

2 | EXPERIMENTAL PROCEDURES AND RESULTS

2.1 | Culture preparation

To set up the ex-ovo chicken embryo culture, we pre-warmed the DMEM/F-12 media (Gibco, without phenol red) at 37°C in a water bath. In the meantime, we connected a sandstone to an oxygen bottle and let it bubble for at least 10 min in autoclaved, deionized water, to wash off dust and other residues (Figure 2B). To prepare the culture dish for embryos, we poured the pre-warmed DMEM/F-12 media into a silicone-coated (SYLGARD) 15 cm Petri dish (Figure 2A). We placed the Petri dish under a heating lamp and used a thermometer to monitor the temperature, adjusting the height level of the lamp to reach and maintain a temperature between 33 and 35°C (Figure 2B). The cleaned sandstone was then

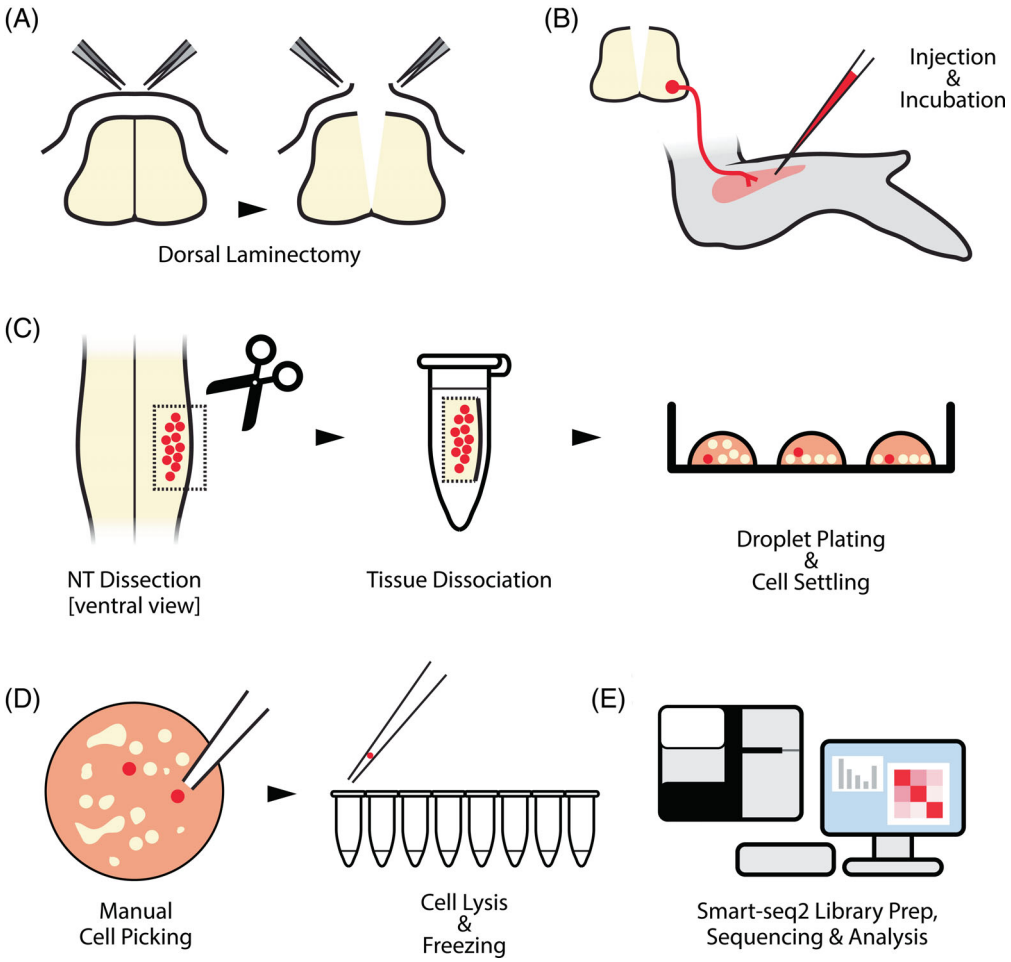

FIGURE 1 Complete workflow of the method. (A) Schematic representing the dorsal laminectomy to ensure good oxygenation of the spinal neurons. The dorsal part of the vertebra is removed, together with the opening of the roof plate. (B) A fluorescent tracer (eg, CTB-555) is injected into the target muscle and embryos are incubated for 5 hours in ex-ovo culture, allowing the fluorescent tracer to be transported to the soma of spiral motor neurons. (C) After backfill culturing, the neural tube is dissected. The success of retrograde tracing is assessed under stereomicroscope and fluorescent neural tissue is isolated. Following papain dissociation, the cells are resuspended and plated in Neurobasal plating media for subsequent manual purification. (D) Healthy-looking fluorescent cells are separated from debris and nonfluorescent cells by aspiration. Once the cells are washed in PBS, they are transferred into lysis buffer in a single tube of a PCR strip on ice. Lysed cells can be kept at −80°C until further processing. (E) Smart-seq2 libraries are prepared and sequenced, and the obtained cell transcriptomes are checked for overall quality and analyzed to detect the expression of specific marker genes

placed in the media and let to bubble thoroughly during the time of dissection and muscle injection.

2.2 | Embryo dissection and limb muscle injection

White Leghorn chicken eggs (*Gallus gallus*) were incubated at 38°C with 60% humidity for 9 days. We gently cracked the egg and poured the content into a glass dish. We then transferred the embryo into a PBS dish, in order to wash all the yolk off, decapitated the embryos, and put it into a black silicone-coated dish (Figure 2A). Ventral side down, we pinned the embryos to the dish by the neck and the tail and made a transversal cut of the spinal cord at the middle of the back, approximately at the level of the last pair of ribs. After checking the entire spinal cord was cut through, we then skinned the back to perform a dorsal laminectomy (Figure 1A). Indeed, at late embryonic stages, it is important to ensure proper oxygenation of spinal neurons. To do so, using forceps, we removed the dorsal part of the vertebra, starting from the caudal part up to the neck while making sure that the underlying spinal cord remains intact. Finally, with a fire-sharpened Tungsten needle, we opened the roof plate for better oxygenation of the ventral spinal neurons during the incubation period. Once the dorsal laminectomy was performed, the

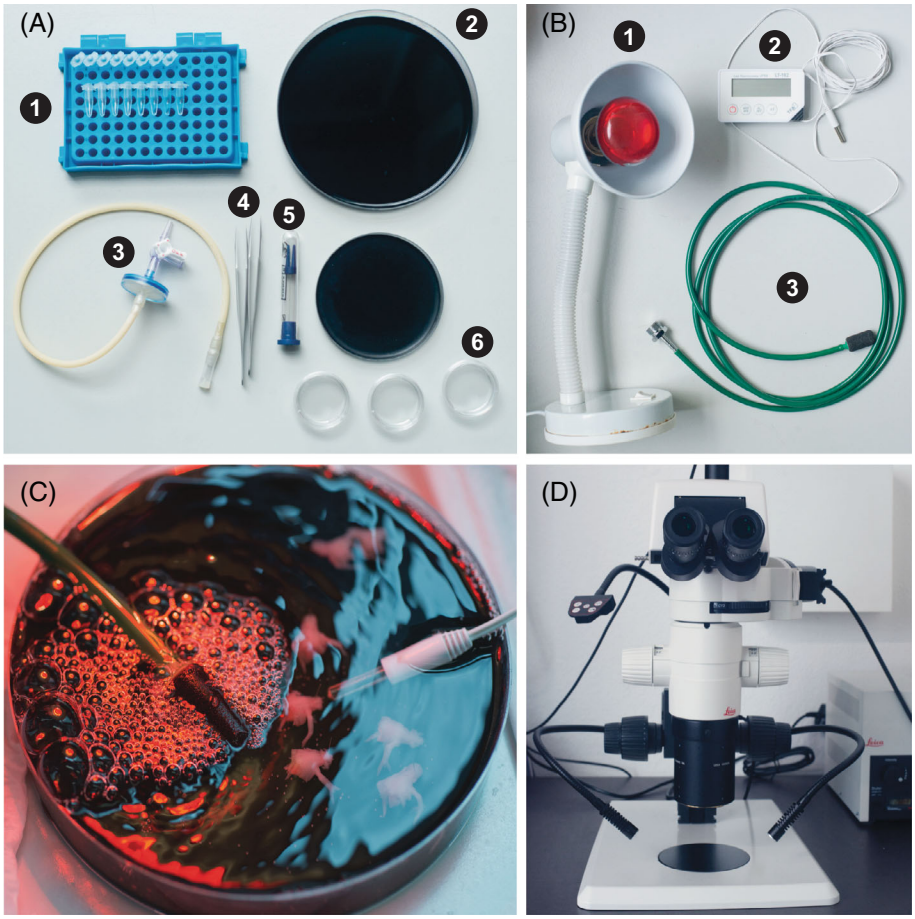

FIGURE 2 Inventory of tools and equipment required. (A) (1) PCR tubes, if possible, with individual lids (Eppendorf), (2) two black SYLGARD coated Petri dishes (10 cm and 15 cm), (3) mouth pipette with a syringe filter and valve to control the flow rate, (4) dissection forceps (FST size 55), (5) sterile micropipettes (ORIGIO MBB-FP-M-0), and (6) clear 6 cm Petri dishes for PBS washes. (B) (1) Heating lamp to maintain culture temperature, (2) thermometer, and (3) sandstone connected via a plastic tube and valve regulator to a pressurized oxygen bottle. (C) Image of embryos in culture during retrograde labeling experiment. The sandstone provides oxygenation, and the temperature is monitored during the entire incubation time. (D) Fluorescent stereomicroscope (Leica MZ10 F, with 1.6× ApoPlan lens, connected to a Leica EL6000 fluorescent light source) used for cell picking

lumbar part with the legs of the embryos could then be removed and discarded.

For limb muscle injection, we pinned the embryo on its side at the level of the neck for better visibility and accessibility of the wing muscles. In this proof of principle experiment, we decided to focus on the EMR and the FDQ, a dorsally and ventrally located wing muscles, respectively.[23,24] Without damaging the muscle bundles, we delicately skinned the forearm. Using a mouth pipette and pulled capillary, we injected a fluorescently labeled tracer molecule, Cholera Toxin Subunit B (CTB-555, 0.1 mg/mL in PBS, Invitrogen), into the target muscle, that is, the EMR or FDQ. If multiple injections are possible all along with the bigger muscle like the EMR, it is important to keep its structure intact and avoid leakage of the tracer into adjacent muscles (Figure 3A). However, a particular focus should be given to injections at the mid-section of the fusiform muscle, as most motor neuron axon termini contact the muscle there (Figure 3B).

After injection, we put the embryos in the previously oxygenated culture dish with pre-warmed DMEM/F-12 media and pinned them down (Figure 2C). During the 5 hours of incubation, we kept on monitoring the temperature, checked for proper oxygenation, and supplemented the dish with fresh, prewarmed media if needed, in order to keep the embryos submerged.

2.3 | Retrograde axonal labeling quality check

Once the incubation time was up, we closed the oxygen bottle and washed the sandstone in autoclaved water until the oxygen stopped running. To isolate the spinal cord, we pinned the embryos face down to a new silicone-coated Petri dish and gently pass closed forceps underneath the neural tube, to release it from its enclosing of the forming vertebrae. Special care had to be taken since the targeted motor neurons are located in the ventral horn, that is, directly above where the spinal cord was released from. The neural tube was pinned down with its ventral side up and inspected for successful backfill. To do so, we placed the dish under binoculars equipped with fluorescent lamps and adequate filters (Figure 2D). In case the axonal tracing was successful, we observed a fluorescent signal in the ventral horn of the spinal cord (Figure 3C). Under the scope, we microdissected only the fluorescent part of the neural tube

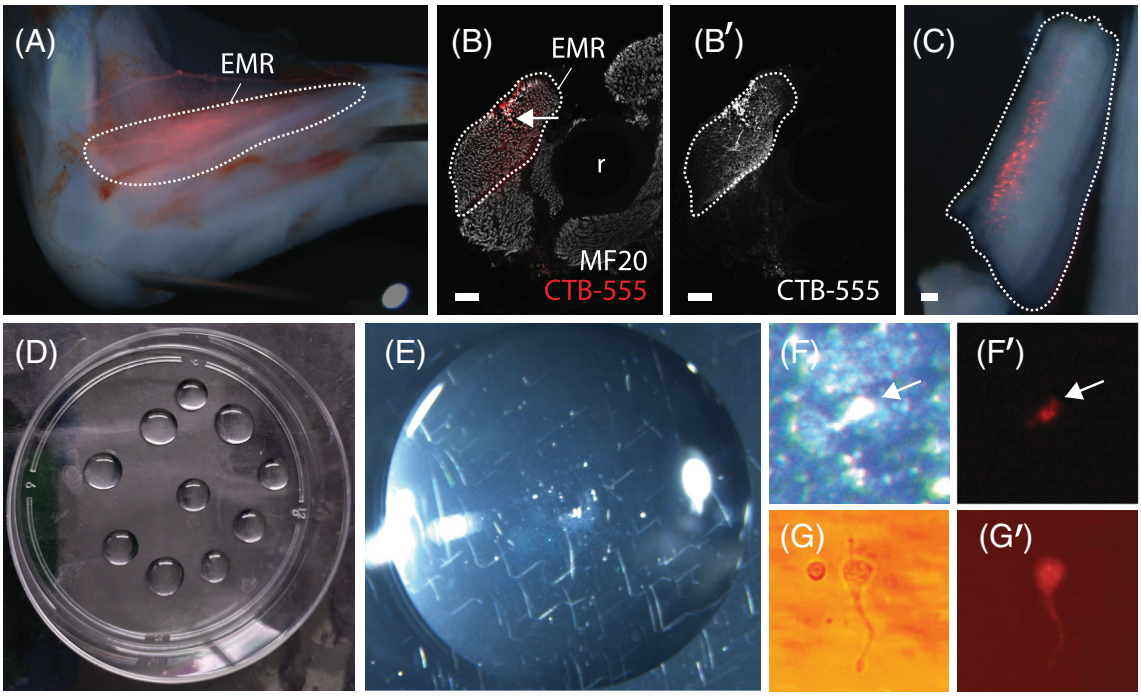

FIGURE 3 Retrograde labeling and EMR muscle injection quality check. (A) CTB-555 injection site in the EMR muscle. The white dotted line shows the extent of the muscle. (B) Transversal cross-section of an injected limb with muscles in gray (MF20). The white dotted line shows the EMR muscle and the white arrow points to deformities at the injection site, r for radius. (B′) Fluorescent image of the CTB-555 injection site in the EMR muscle with no signal in adjacent muscles. (C) Fluorescent signal in the ventral neural tube after retrograde labeling. The white dotted line shows the dissected portion of the neural tube. (D) The post-dissociation cell suspension is plated in drops. (E) Close-up image of a drop of cell suspension. Note that most of the cells are grouped in the middle of the drops. (F and F′) Bright field and fluorescent image of a red fluorescent plated cell. Note the concentration of cells and debris at this first stage of cell picking. The white arrow is showing a single labeled cell. (G and G′) Bright field and fluorescent image of a single isolated red fluorescent cell after several rounds of PBS washes. We can even observe the axon projection of the neuron

(Figure 3C) and placed it in a labeled 2 mL Eppendorf tube with PBS. As they might alter the efficiency of the tissue dissociation, we eliminated all residues present in the culture media by washing the dissected tissue twice with PBS. For an additional injection quality control, we dissected the injected limb, fixed it in PFA 4% overnight, and transversally sectioned it at the correct proximo-distal level, then stained it for Myosin heavy chain (MF20; 1:500, DSHB) to visualize proper CTB-555 injection inside of the targeted muscle (Figure 3B).

2.4 | Neural tube dissociation and cell plating

Neurons, and neuronal tissues in general, are particularly sensitive to tissue dissociation, especially after prolonged periods of ex-ovo incubation. Therefore, a mild papain dissociation method was performed, and dissociated cells were plated in a neuron-specific media (plating media: Neurobasal Gibco, 5% fetal bovine serum [FBS] and 1% GlutaMAX Gibco).[25] One hour and a half before the end of the incubation period required for axonal tracing, we put the Neurobasal plating media in a Petri dish inside a cell culture incubator for CO_2 equilibration. Additionally, half an hour before the end, we mixed FACSmax (Amsbio) dissociation media with papain (Roche) to get a 0.25 mg/mL final concentration of the enzyme. We pre-warmed the mix in a water bath at 37°C until the neural tube was completely dissected. For tissue trituration, we used a P1000 pipette and prepared for each sample the following filtered tips: one pipette cut close to the 250 µL mark, and a second one cut halfway between the 250 µL mark and the end of tip to have a smaller opening. Both pipette tips were flamed briefly, to soften the sharp edges. Additionally, we prepared two more uncut pipette tips for further trituration. After spraying them with ethanol, we placed them under the cell culture hood.

Once the desired piece of neural tissue was dissected, we discarded the PBS to add 1 mL of dissociation media per sample and put them in a water bath at 37°C for 10 minutes, combining it with a gentle flicking step after 5 minutes. With the first cut pipette tip, we triturated the tissue by gently pipetting 20 times up and down, and

then placed the sample back at 37°C for an additional 5 minutes. The last step was repeated with the second cut and the uncut pipette tips, until no visible tissue clumps remained present.

The samples were centrifuged at 300 × *g* for 7 minutes at room temperature. After discarding the supernatant, we resuspended the cell pellet in 600 μL of plating media. Typically, the dissociation of a single spinal cord only gave a small number of cells (around 300,000 cells/mL, with a cell viability of about 90%, as evaluated by Cellometer [Nextcelom Bioscience]). Plating of single drop of ~150 μL of cell suspensions in a bigger Petri dish provided a higher concentration of cells per surface area than covering the entire dish with the cell suspension (Figure 3D). This substantially facilitated the detection and manual purification of fluorescent cells afterwards. We deposited the cell suspension drops in a 10 cm Petri dish and placed them in a cell culture incubator for at least 30 minutes, so that cells had time to settle at the bottom of the drops (Figure 3D,E).

2.5 | Manual cell isolation

First, we prepared the workspace for cell selection and picking, by cleaning all surfaces, instruments, and tools with RNAseZap RNAse inhibitor (Invitrogen). As the plating media contain FBS, which may alter the cell lysis process, picked cells must be washed at least twice in clean, cold PBS before depositing them into the lysis buffer. For these washing steps, we first prepared at least three 3 cm Petri dishes right before proceeding with the cell picking. The dishes and the upturned lids were filled with ice-cold PBS. The first Petri dish was then used to fill the capillary with clean PBS, the second one to eject any liquid between picked cells, and the third one to quickly wash the needle (Figure 2A). The PBS-filled lids were used to wash the picked cells as they are shallower and therefore more convenient to pass from one to the other.

To prepare the cellular extracts for Smart-seq2 single-cell RNA-sequencing, we used a cell lysis buffer compatible with this workflow (0.2% (vol/vol) Triton X-100 and 2 U/μL RNase inhibitor).[22] In labeled PCR strips, we put 2.3 μL of lysis buffer in each tube and kept the buffer cooled before and during the experiment on a metal cooling rack on ice.

We assembled the cell aspirator, consisting of a three-way stopcock, a 0.3 μm syringe filter, a cell aspirator tube, and sterile micropipette (Origio, MBB-FP-M-0), and made sure that all seals were tight (Figure 2A). To check if there were no leaks of air and the liquid was properly entering, we put the sterile capillary at the end of the cell aspirator and aspirated PBS. If a leakage of air was observed, we used paraffin sheets and changed the filter, whenever necessary.

When the set-up was ready, we screened the drops of cell suspension under a fluorescent stereomicroscope and roughly approximated the total number of fluorescent cells. We first took up clean PBS into the needle, to reduce capillary action and have improved control over the suction flow. We then aspirated the targeted fluorescent cells spotted in the cell suspension (Figure 3E,F-F′). At this stage, the isolation of a unique cell of interest is almost impossible. Thus, several rounds of PBS washes are required, in order to ensure the transfer of individual cells into the lysis buffer-filled PCR strips. First, we gently ejected the content of the needle into a PBS-filled Petri dish lid. For this, the focus of the binocular was properly adjusted, and to avoid the cells floating out of the field of vision, the ejection was carried out very slowly. After checking for the presence of the fluorescent cell by turning off the bright field light source, we washed the capillary needle, then re-aspirated the neuron with as few other, nonfluorescent cells as possible. We repeated the previous steps and blew clean PBS around the CTB-555-positive cell, in order to wash away any remaining cells and debris from its surroundings. These washing steps must be repeated as much as needed, using the 3 cm Petri dishes and their upturned lids previously filled with ice-cold PBS, until a single cell is obtained in a completely isolated fashion. A final check should be carried out, with both bright field and fluorescent light sources. Finally, we washed the capillary with PBS again and we aspirated a unique target cell and put it into a PCR stripe tube containing the lysis buffer.

We repeated the process of cell picking until there were no fluorescent cells left in the drops. It is important to note down any observations about the individual picked cells, for example, their shape, relative size to other cells, and fluorescence intensity. All those parameters will be considered, when deciding which resulting cDNA samples will eventually be selected for the following library preparation and sequencing steps. A good example of a healthy-looking motor neuron, with its axon still visible, is shown in Figure 3G-G′. The PCR stripes were then stored at −80°C, until cDNA production and subsequent library preparation.

2.6 | Library preparation, sequencing, and representative results

After reverse transcription (Superscript II) and amplification (Invitrogen), each individual cDNA sample was loaded onto a Fragment Analyzer (Agilent) for quality

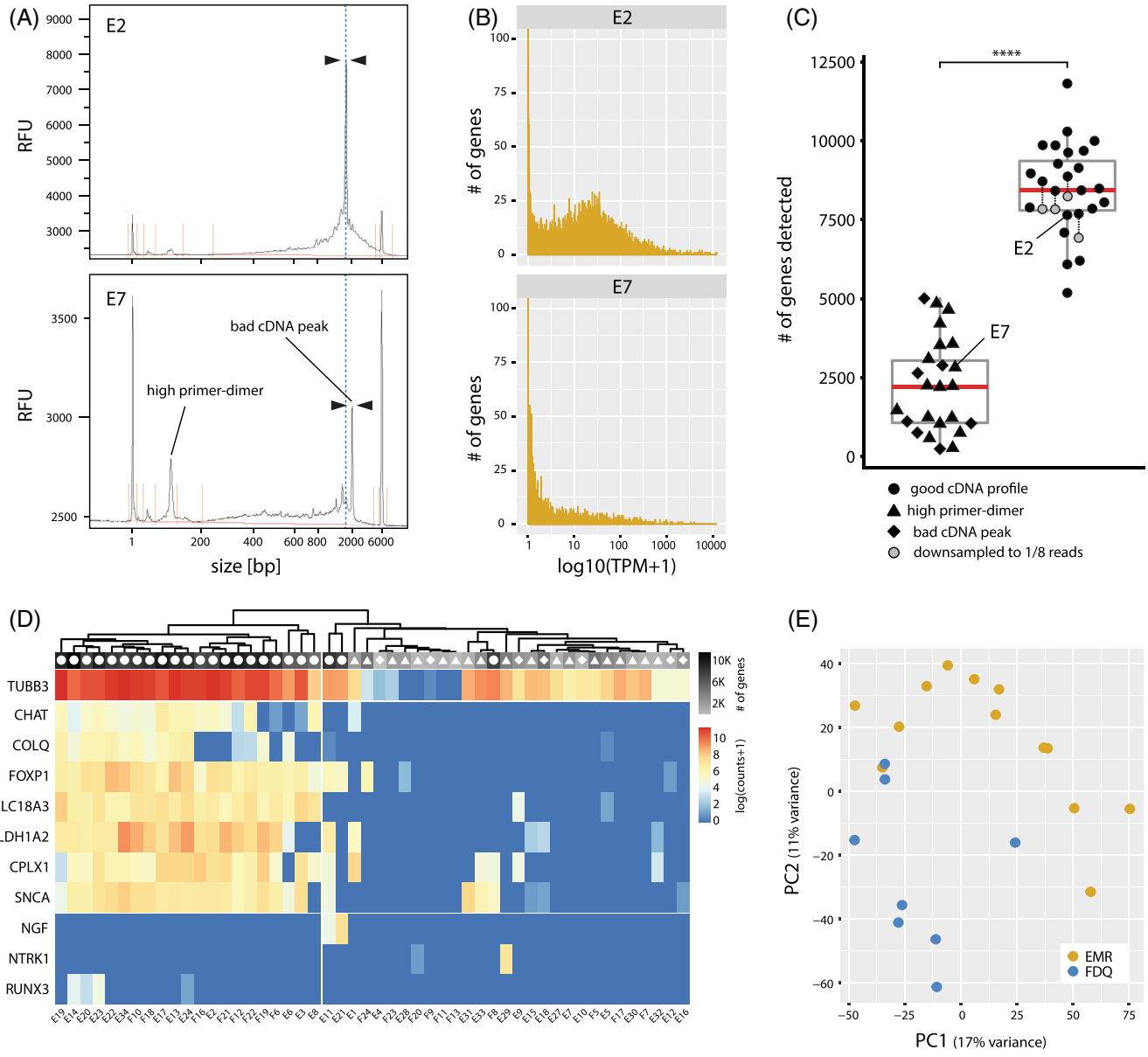

FIGURE 4 Representative results of individual neuron sequencing. (A) Fragment Analyzer cDNA profiles of two individual cells (E2 and E7). The top panel shows the profile of a high-quality cell, with a main peak around 1650 to 1700 bp (black arrowheads, approximately 8000 RFUs).The bottom panel shows the profile of a low-quality cell with the main peak fainter shifted toward 2000 bp (black arrowheads, 3000 RFUs) and the relative primer-dimer concentration is higher. (B) TPM (transcript per million) distribution in a high-quality cell (E2) and low-quality cell (E7). (C) Box plot representing the number of genes detected per sample. Different quality assessments of cDNA profiles are represented by different geometric shapes (circles, triangles, and diamonds). Samples with a good cDNA profile show a significantly higher number of genes detected (Wilcoxon rank sum test, $P < .0001$). (D) Heat map of selected marker transcript numbers. Cells are grouped by unsupervised hierarchical clustering (muscle connectivity labeled by E: EMR and F: FDQ). The overall number of genes detected per cell is indicated by grayscale, and the quality of their cDNA profiles by different geometric shapes (see legend of panel C). (E) Principal component analysis (PCA) of gene expression levels of motor neurons innervating EMR and FDQ, based on the top 500 most variably expressed genes

assessment. Genomic libraries were then prepared from selected cDNA samples using an Illumina Nextera XT kit. All libraries were sequenced on an Illumina Novaseq 6000 SP Sequencer (100 cycles, 50 bp paired-end reads), to a depth of 2.5 to 21.3 million reads per sample. The raw reads were trimmed with Trimmomatic (v.0.39), using the Illuminaclip parameter with the distributed Nextera adapter file, aligned with STAR (v.2.5.2) to the GRCg6a chicken genome, and count tables were created with HTSeq (v.0.6.1).[26-28]

Retrospectively, with the sequencing results of our proof-of-principle experiment at hand, we were able to define cDNA quality metrics that were predictive of sequencing success. Namely, to assess Fragment Analyzer cDNA profile as a potential predictor of expected gene expression library complexity, we correlated the presence/absence of a "bad cDNA peak" and/or "high primer-dimer" content (Figure 4A) with the overall number of genes detected, and their expression level distribution (Figure 4B,C). For example, good-quality cells like sample "E2" were characterized by a cDNA profile containing an overall high peak between 1.6 and 1.7 kb (full-length transcripts), and a small number of fragments below 500 bp. Moreover, only a small peak of primer dimers around 100 bp was visible (Figure 4A, top panel). Contrary to this, in cells yielding low quality transcriptomes like sample "E7" (see Figure 4B,C), a substantially weaker main peak was detected (~3000 Relative Fluorescent Units [RFUs] for "E7" vs ~8000 RFUs for "E2"), reflecting overall lower RNA concentration, and the peak was shifted toward 2 kb (Figure 4A, see blue dotted line for reference). Furthermore, a higher primer-dimer peak was detected in those cells (Figure 4A, bottom panel). After sequencing and transcript quantification, cells with a good cDNA profile presented a bimodal distribution of individual gene expression levels, whereas poor cDNA profiles resulted in a post-sequencing transcript level distribution skewed toward zero (Figure 4B, compare top graph for sample "E2" to bottom one for sample "E7"). Moreover, an overall significantly higher number of genes was detected (8000-12,000 genes) in cells presenting a good cDNA profile, even after down-sampling the number of reads per sample to 1/8 of the original count (Figure 4C, grey circles). However, some samples presented a more puzzling cDNA profile, showing an overall decent cDNA profile—according to the previously defined criteria—but with a slightly more pronounced proportion of shorter fragments (<700 bp) indicative of RNA degradation. Post sequencing, we detected mostly mitochondrial gene transcripts at a high level in these cells, but low expression levels for most other genes. These results thus convinced us that the amount of small (below 500 bp) must also be considered as a criterion, in addition to cDNA peak height and position, and primer-dimer content. In summary, Fragment Analyzer cDNA profiles are a reliable predictor of the number of genes detected after sequencing, which are key indicators of transcriptome information content. As such, a sample selection step based on Fragment Analyzer cDNA profiles before library preparation and sequencing can maximize information gain and reduce overall costs, to streamline the overall efficiency of our experimental workflow.

In order to validate the identity of the sequenced cells as motor neurons, a number of marker gene expression profiles were examined using an expression heatmap plot and unsupervised hierarchical clustering (Figure 4D). Almost all cells expressed the general neuronal differentiation marker *TUBB3* (*TUJ1*). However, cells of the left-most cluster showed a higher transcript count for *TUBB3*, and an overall higher number of genes detected than for the other cluster (greyscale, above). Interestingly, the majority of cells (21 out of the 24) presenting a good cDNA profile, expressed Choline Acetyltransferase (*CHAT*), Acetylcholinesterase subunit Q (*COLQ*), and Vesicular Acetylcholine Transporter (*SLC18A3*), three gene members of the biosynthesis and transport chain of the motor neuron-specific neurotransmitter acetylcholine.[29] *CPLX1* and *SCNA*, both known to be involved in the modulation of neurotransmitter action and implicated in motor neuron diseases were also expressed by these cells.[30,31] Furthermore, the cells also expressed *FOXP1* and *ALDH1A2*, two well-known embryonic marker genes of developing LMC motor neurons (left most cluster in Figure 4D).[32,33] To exclude the possibility of contamination by dorsal root ganglia cells, which are also labeled during axonal backfill procedures, we additionally checked for the expression of sensory neuron marker genes. As expected, none of the sequenced cells did express any sensory neuron markers like *NGF*, *NTRK1*, or *RUNX3*[34,35] at substantial levels, thereby validating our micro-dissection procedure and the fact that the purified cells indeed represent motor neurons coming from the ventral part of the neural tube.

Finally, to assess the ability of our method to transcriptionally differentiate closely related motor neuron subtypes, we compared our data sets of motor neurons connected to two different muscles, the EMR and FDQ, using principal component analysis (PCA) of levels of gene expression. PCA was performed with zinbwave (v.1.12.0) and DESeq2 (v.1.30.0),[36,37] following the respective vignettes' suggestions concerning data transformation and normalization, and using the top 500 most variably expressed genes. On the resulting PCA plot, cellular transcriptomes coming from motor neurons with the same muscle connection appear to cluster together, with a striking separation between the EMR and FDQ motor neuron subsets (Figure 4E). This result demonstrates that our method can reliably detect even minor transcriptional profile differences between closely related motor neuron subsets, which reflects their axonal connections to distinct muscle groups.

Collectively, the following criteria should thus be taken into account, when deciding which cDNA samples to include for library preparation and sequencing, as well as downstream bioinformatics analyses: (1) high cDNA

concentration (>5 μg/μL), with a cDNA profile peak at a size of 1.5 to 1.7 kb and a low proportion of short fragments and primer-dimers; (2) less than ~50% of mitochondrial gene transcripts per cell; (3) more than 6000 genes detected per cell; (4) expression of motor neuron markers such as *CHAT*, *SLC18A3*, *FOXP1*; and (5) absence of sensory neuron markers expression like, for example, *NGF*, *NTRK1*, and *RUNX3*. Samples meeting all these criteria should generally provide robust and reliable information on the transcriptome of motor neurons connected to a particular muscle group, although certain samples meeting only some of the criteria above might be also considered, on a case-by-case basis, to determine whether their inclusion into further analyses is reasonable.

3 | DISCUSSION AND CONCLUSION

Here, we present a method that successfully combines the classical experimental embryology technique of retrograde axonal tracing with state-of-the-art single-cell RNA-sequencing technology of individual motor neurons, in order to investigate motor neuron pool- and muscle target-specific transcriptomes at individual cell resolution. Our procedure proved efficient not only in detecting motor neuron specific marker gene expression profiles in EMR- and FDQ-connected cells, but also in correlating their respective cDNA metrics to the eventual expected transcriptome quality. Importantly, this procedure can also be used to compare other set of neurons innervating various muscle targets located in different parts of the embryo.

Ex-ovo manipulation and culturing of chicken embryos can be performed more easily at earlier stages (ie, before Hamburger-Hamilton stage HH34, or embryonic day 8) without the need for invasive surgery. The transcriptional logic of the early dorsal-ventral choice point could thereby already be addressed via the dorsal or ventral retrograde labeling of axonal projections. Unfortunately, muscle-specific resolution cannot be achieved at these early stages of muscle formation, due to the absence of fully individualized muscle bundles. For mid-gestation chicken embryos (ie, between Hamburger-Hamilton stage HH34 and HH36, or embryonic day 8 and day 10, when individual muscle bundles have formed), our culture conditions required the optimization of various parameters. Indeed, retrograde axonal labeling at limb levels is influenced by multiple factors, such as the age of the embryo, the size of the muscle, and its position along the proximo-distal axis of the developing limb. Later stage embryos are more difficult to culture, due to their increased size, the reduced diffusion rates to the targeted motor neurons, the formation of vertebral cartilage, and the thickening of the skin. Previous studies described ex-ovo retrograde labeling methods using the more difficult ventral laminectomy which involves the evisceration of the embryo and the detachment of the ventral part of the vertebra.[17] However, this type of anatomical surgery only seems necessary for embryo culture experiments that go beyond day 10 (stage HH36). In this case, an in-ovo approach should also be considered. Owing to the constrained accessibility of the anterior body part—which is due to the turning of the chick embryo, these studies would likely have to be restricted to the muscles of the hindlimb.[38] In our study, we propose to use a less invasive technique, the dorsal laminectomy, allowing us to preserve as much as possible the ventral part of the neural tube while ensuring better oxygenation of the tissue, motor neuron survival, and thereby making a successful axonal tracing more likely. Since the emergence of the retrograde labeling technique in the 1970s in chicken, they have also been extended to mouse embryos, to study neuronal connections at mid-gestation (around 12 days of development). Our study raises the intriguing possibility that the optimized protocol for culturing embryos at later stages could also allow for a transfer of retrograde labeling to later-stage mouse embryology studies.

The overall success of our retrograde labeling method also depends on the target to be injected, and the axonal distance to the neuron cell bodies. Comparing our test studies on the proximal EMR and the distal FDQ muscles, we noticed that smaller and more distally located limb muscles, such as the autopodial FDQ, are far more difficult to properly inject because of their size and elongated shape. Moreover, retrograde transport also becomes less reliable, due to the increased distance between the injected muscle and its connected motoneurons. Indeed, we observed a lower number of fluorescently labeled cells with the smaller and more distal muscles compared to the bigger, domed, and proximal ones. These observations suggest that the number of retrograde labeling experiments would have to be increased, in order to successfully pick a decent number of cells connected to the more distally located and smaller muscle groups and other systems. However, as shown in Figure 4, we were still able to reliably backfill and trace the axons of both subsets of motor neurons, connecting either to the larger, proximally located EMR muscle, as well as for the thinner, distally located FDQ muscle.

The handling of single cells, in order to reliably pick them as individual entities, can appear difficult. Indeed, multiple rounds of successive washes in PBS have proved critical to ensure the picking of single cells. For future

users, generic fluorescent cell markers such as Bio-Tracker dyes (Sigma-Aldrich), labeling cell membrane, or Sytox (Invitrogen), indicating dead cells, might be an option to consider, in order to help the experimenter visualize all cells, and differentiate them from the retrograde-labeled ones. Alternatively, the use of the ubiquitous GFP transgenic lines could be considered.[39,40]

Overall, in our test data set, only 21 of 50 cellular transcriptomes (42%) could unequivocally be identified as originating from motor neurons, based on their gene expression signatures related to the cholinergic pathway and other motor neuron marker genes. However, with our retrospective analysis of cDNA profiles and resultant transcriptome quality, we now have a unique checklist of cDNA quality metrics for future studies. This checklist allows the interested researcher to only select samples whose cDNA profiles pass these criteria to proceed with library preparation and sequencing. For example, from the 50 cDNA profiles generated in this study, only 24 would now be deemed of sufficient quality for library preparation and sequencing (see circles, Figure 4C,D), thereby increasing the percentage of successful motor neuron transcriptomes obtained from 42% to 88% (21 of 24). Nevertheless, the aforementioned percentages can still be considered as a rough guideline for experimental design, when determining the overall number of cells to be purified to obtain a certain number of high-quality cDNA profiles and, by extension, single motor neuron transcriptomes.

Finally, in the era of single-cell sequencing, it has become essential for neurobiologists not only to study the transcriptomes of individual motor neurons, but also to correlate these molecular signatures with their eventual axonal projection patterns. To do so, techniques combining single-cell sequencing with retrograde labeling have already been developed in recent years, in order to decipher the transcriptional logic of neuronal wiring. Most of these studies, however, were performed in early postnatal or adult mice, using virus or CTB injections.[41-44] While these approaches do offer superior labeling efficiency compared to our method and—by extension—higher expected cell numbers, they do so at the expense of temporal resolution. Moreover, they only allow for the probing of developmental time points at which the wiring architecture of neuromuscular circuits has already been well established. Our method presented here opens the possibility to study the dynamics of the system at finer temporal resolution and at much earlier developmental time points, when individualized muscle bundles are just about to establish their connections with incoming motor neuron axons. As such, it will likely help to uncover motor neuron transcriptome signatures relevant for early neuromuscular circuit formation, as well as probe the potential plasticity within the system following pharmacological, genetic, or embryological manipulations.[24,44]

In conclusion, here we present an experimental workflow to investigate muscle target-specific transcriptional signatures of single motor neurons. Through the combination of axonal backfilling with individual cell picking and Smart-seq2 single-cell RNA-sequencing, we demonstrate its ability to generate high-quality transcriptomes of single motor neurons in a pool-specific manner, with known target muscle connectivity. Importantly, by combining it with transcriptional profiling of other involved tissue types, for example, muscles, data produced with our approach may lay the foundation for a comprehensive and integrative understanding of the transcriptional logic underlying motor neuron cell type specification and differentiation, as well as neuromuscular circuit assembly and refinement.

AUTHOR CONTRIBUTIONS

Bianka Berki: Conceptualization (equal); formal analysis (equal); investigation (equal); methodology (equal); validation (equal); visualization (equal); writing – original draft (equal); writing – review and editing (equal). **Fabio Sacher:** Data curation (equal); formal analysis (equal); investigation (equal); methodology (equal); validation (equal); visualization (equal); writing – review and editing (equal). **Antoine Fages:** Formal analysis (equal); methodology (equal); validation (equal); visualization (equal); writing – review and editing (equal). **Patrick Tschopp:** Conceptualization (equal); data curation (equal); formal analysis (equal); funding acquisition (equal); investigation (equal); methodology (equal); project administration (equal); supervision (equal); validation (equal); visualization (equal); writing – review and editing (equal). **Maëva Luxey:** Conceptualization (equal); data curation (equal); formal analysis (equal); funding acquisition (equal); investigation (equal); methodology (equal); supervision (equal); validation (equal); visualization (equal); writing – original draft (equal); writing – review and editing (equal).

ACKNOWLEDGMENTS

The authors wish to thank Elodie Burcklen and Christian Beisel at the "Genomics Facility Basel" for help with library preparation and sequencing, and all members of our group for useful discussions. All calculations were performed at sciCORE (http://scicore.unibas.ch/), the scientific computing center at the Universität Basel. This work was supported by a grant of the *Forschungsfonds* of the Universität Basel to ML, and research funds from the *Olga Mayenfisch Stiftung*, the *Fondation Suisse de Recherche sur les Maladies Musculaires* (FSRMM), the Swiss National Science Foundation (SNSF project grant

31003A_170022), and the Universität Basel to PT. Open access funding provided by Universitat Basel.

DATA AVAILABILITY STATEMENT

Raw sequencing data are available under GEO accession number GSE203595.

ORCID

Patrick Tschopp https://orcid.org/0000-0001-7339-3990
Maëva Luxey https://orcid.org/0000-0003-2752-8756

REFERENCES

1. Sagner A, Briscoe J. Establishing neuronal diversity in the spinal cord: a time and a place. *Development*. 2019;146(22):dev182154. doi:10.1242/dev.182154
2. Arber S, Ladle DR, Lin JH, Frank E, Jessell TM. ETS gene Er81 controls the formation of functional connections between group Ia sensory afferents and motor neurons. *Cell*. 2000;101(5):485-498. doi:10.1016/S0092-8674(00)80859-4
3. Dasen JS, Tice BC, Brenner-Morton S, Jessell TM. A Hox regulatory network establishes motor neuron pool identity and target-muscle connectivity. *Cell*. 2005;123(3):477-491. doi:10.1016/j.cell.2005.09.009
4. Price SR, De Marco Garcia NV, Ranscht B, Jessell TM. Regulation of motor neuron pool sorting by differential expression of type II cadherins. *Cell*. 2002;109(2):205-216. doi:10.1016/S0092-8674(02)00695-5
5. Price SR, Briscoe J. The generation and diversification of spinal motor neurons: signals and responses. *Mech Dev*. 2004;121(9):1103-1115. doi:10.1016/j.mod.2004.04.019
6. Demireva EY, Shapiro LS, Jessell TM, Zampieri N. Motor neuron position and topographic order imposed by β- and γ-catenin activities. *Cell*. 2011;147(3):641-652. doi:10.1016/j.cell.2011.09.037
7. Delile J, Rayon T, Melchionda M, Edwards A, Briscoe J, Sagner A. Single cell transcriptomics reveals spatial and temporal dynamics of gene expression in the developing mouse spinal cord. *Development*. 2019;146(12):dev173807. doi:10.1242/dev.173807
8. Blum JA, Klemm S, Shadrach JL, et al. Single-cell transcriptomic analysis of the adult mouse spinal cord reveals molecular diversity of autonomic and skeletal motor neurons. *Nat Neurosci*. 2021;24(4):572-583. doi:10.1038/s41593-020-00795-0
9. Eze UC, Bhaduri A, Haeussler M, Nowakowski TJ, Kriegstein AR. Single-cell atlas of early human brain development highlights heterogeneity of human neuroepithelial cells and early radial glia. *Nat Neurosci*. 2021;24(4):584-594. doi:10.1038/s41593-020-00794-1
10. Rayon T, Maizels RJ, Barrington C, Briscoe J. Single-cell transcriptome profiling of the human developing spinal cord reveals a conserved genetic programme with human-specific features. *Development*. 2021;148(15):dev199711. doi:10.1242/dev.199711
11. Russ DE, Cross RBP, Li L, et al. A harmonized atlas of mouse spinal cord cell types and their spatial organization. *Nat Commun*. 2021;12(1):5722. doi:10.1038/s41467-021-25125-1
12. Blum JA, Gitler AD. Singling out motor neurons in the age of single-cell transcriptomics. *Trends Genet*. Forthcoming 2022. doi:10.1016/j.tig.2022.03.016
13. Kebschull JM, Garcia da Silva P, Reid AP, Peikon ID, Albeanu DF, Zador AM. High-throughput mapping of single-neuron projections by sequencing of barcoded RNA. *Neuron*. 2016;91(5):975-987. doi:10.1016/j.neuron.2016.07.036
14. Han Y, Kebschull JM, Campbell RAA, et al. The logic of single-cell projections from visual cortex. *Nature*. 2018;556(7699):51-56. doi:10.1038/nature26159
15. Hanchate NK, Lee EJ, Ellis A, et al. Connect-seq to superimpose molecular on anatomical neural circuit maps. *Proc Natl Acad Sci USA*. 2020;117(8):4375-4384. doi:10.1073/pnas.1912176117
16. Xu P, Peng J, Yuan T, et al. High-throughput mapping of single-cell molecular and projection architecture of neurons by retrograde barcoded labelling. 2021. doi:10.1101/2021.05.16.444258
17. Landmesser L. The development of motor projection patterns in the chick hind limb. *J Physiol*. 1978;284:391-414.
18. Hollyday M. Organization of motor pools in the chick lumbar lateral motor column. *J Comp Neurol*. 1980;194(1):143-170. doi:10.1002/cne.901940108
19. Hollyday M, Jacobson RD. Location of motor pools innervating chick wing. *J Comp Neurol*. 1990;302(3):575-588. doi:10.1002/cne.903020313
20. Lance-Jones C, Landmesser L, Kuffler SW. Pathway selection by chick lumbosacral motoneurons during normal development. *Proc R Soc Lond B Biol Sci*. 1981;214(1194):1-18. doi:10.1098/rspb.1981.0079
21. Mendelsohn AI, Dasen JS, Jessell TM. Divergent Hox coding and evasion of retinoid signaling specifies motor neurons innervating digit muscles. *Neuron*. 2017;93(4):792-805.e4. doi:10.1016/j.neuron.2017.01.017
22. Picelli S, Faridani OR, Björklund ÅK, Winberg G, Sagasser S, Sandberg R. Full-length RNA-seq from single cells using Smart-seq2. *Nat Protoc*. 2014;9(1):171-181. doi:10.1038/nprot.2014.006
23. Sullivan G. Anatomy and embryology of the Wing Musculature of the domestic fowl (*Gallus*). *Aust J Zool*. 1962;10(3):458-518. doi:10.1071/ZO9620458
24. Luxey M, Berki B, Heusermann W, Fischer S, Tschopp P. Development of the chick wing and leg neuromuscular systems and their plasticity in response to changes in digit numbers. *Dev Biol*. 2020;458(2):133-140. doi:10.1016/j.ydbio.2019.10.035
25. Langlois SD, Morin S, Yam PT, Charron F. Dissection and culture of commissural neurons from embryonic spinal cord. *J Vis Exp*. 2010;39:e1773. doi:10.3791/1773
26. Dobin A, Davis CA, Schlesinger F, et al. STAR: ultrafast universal RNA-seq aligner. *Bioinformatics*. 2013;29(1):15-21. doi:10.1093/bioinformatics/bts635
27. Bolger AM, Lohse M, Usadel B. Trimmomatic: a flexible trimmer for Illumina sequence data. *Bioinformatics*. 2014;30(15):2114-2120. doi:10.1093/bioinformatics/btu170
28. Anders S, Pyl PT, Huber W. HTSeq—a python framework to work with high-throughput sequencing data. *Bioinformatics*. 2015;31(2):166-169. doi:10.1093/bioinformatics/btu638
29. Petrov KA, Proskurina SE, Krejci E. Cholinesterases in tripartite neuromuscular synapse. *Front Mol Neurosci*. 2021;14:811220. doi:10.3389/fnmol.2021.811220
30. Drew CJG, Kyd RJ, Morton AJ. Complexin 1 knockout mice exhibit marked deficits in social behaviours but appear to be

cognitively normal. *Hum Mol Genet*. 2007;16(19):2288-2305. doi:10.1093/hmg/ddm181
31. Kline RA, Kaifer KA, Osman EY, et al. Comparison of independent screens on differentially vulnerable motor neurons reveals alpha-synuclein as a common modifier in motor neuron diseases. *PLoS Genet*. 2017;13(3):e1006680. doi:10.1371/journal.pgen.1006680
32. Dasen JS, De Camilli A, Wang B, Tucker PW, Jessell TM. Hox repertoires for motor neuron diversity and connectivity gated by a single accessory factor, FoxP1. *Cell*. 2008;134(2):304-316. doi:10.1016/j.cell.2008.06.019
33. Bonanomi D. Axon pathfinding for locomotion. *Semin Cell Dev Biol*. 2019;85:26-35. doi:10.1016/j.semcdb.2017.11.014
34. Faure L, Wang Y, Kastriti ME, et al. Single cell RNA sequencing identifies early diversity of sensory neurons forming via bipotential intermediates. *Nat Commun*. 2020;11(1):4175. doi:10.1038/s41467-020-17929-4
35. Wu H, Petitpré C, Fontanet P, et al. Distinct subtypes of proprioceptive dorsal root ganglion neurons regulate adaptive proprioception in mice. *Nat Commun*. 2021;12(1):1026. doi:10.1038/s41467-021-21173-9
36. Love MI, Huber W, Anders S. Moderated estimation of fold change and dispersion for RNA-seq data with DESeq2. *Genome Biol*. 2014;15(12):550. doi:10.1186/s13059-014-0550-8
37. Risso D, Perraudeau F, Gribkova S, Dudoit S, Vert JP. A general and flexible method for signal extraction from single-cell RNA-seq data. *Nat Commun*. 2018;9:284. doi:10.1038/s41467-017-02554-5
38. McGrew MJ, Sherman A, Ellard FM, et al. Efficient production of germline transgenic chickens using lentiviral vectors. *EMBO Rep*. 2004;5(7):728-733. doi:10.1038/sj.embor.7400171
39. Davey MG, Balic A, Rainger J, Sang HM, McGrew MJ. Illuminating the chicken model through genetic modification. *Int J Dev Biol*. 2018;62(1–2-3):257-264. doi:10.1387/ijdb.170323mm
40. Tasic B, Yao Z, Graybuck LT, et al. Shared and distinct transcriptomic cell types across neocortical areas. *Nature*. 2018;563(7729):72-78. doi:10.1038/s41586-018-0654-5
41. Golan N, Kauer S, Ehrlich DB, Ravindra N, Dijk D van, Cafferty WB. Single-cell transcriptional profiling of the adult corticospinal tract reveals forelimb and hindlimb molecular specialization. 2021. doi:10.1101/2021.06.02.446653
42. Baek M, Menon V, Jessell TM, Hantman AW, Dasen JS. Molecular logic of spinocerebellar tract neuron diversity and connectivity. *Cell Rep*. 2019;27(9):2620-2635.e4. doi:10.1016/j.celrep.2019.04.113
43. Zampieri N, Jessell TM, Murray AJ. Mapping sensory circuits by anterograde trans-synaptic transfer of recombinant rabies virus. *Neuron*. 2014;81(4):766-778. doi:10.1016/j.neuron.2013.12.033
44. Velten J, Gao X, Van Nierop Y, Sanchez P, et al. Single-cell RNA sequencing of motoneurons identifies regulators of synaptic wiring in *Drosophila* embryos. *Mol Syst Biol*. 2022;18(3):e10255. doi:10.15252/msb.202110255

How to cite this article: Berki B, Sacher F, Fages A, Tschopp P, Luxey M. A method to investigate muscle target-specific transcriptional signatures of single motor neurons. *Developmental Dynamics*. 2023;252(1):208-219. doi:10.1002/dvdy.507